IAC-12,C1,3,3,x13767

CLUSTER-KEEPING ALGORITHMS FOR THE SAMSON PROJECT

Leonel Mazal,*and Pini Gurfil†
Technion–Israel Institute of Technology, Haifa 32000, Israel

Abstract

Space Autonomous Mission for Swarming and Geolocation with Nanosatellites (SAMSON) is a new satellite mission, led by the Distributed Space Systems Lab at the Technion – Israel Institute of Technology. SAMSON will include three nanosatellites, built based on the CubeSat standard. The mission is planned for at least one year, and has two main goals: (i) Demonstrate long-term autonomous cluster flight of multiple satellites, and (ii) Determine the position of a radiating electromagnetic terrestrial source based on time difference of arrival (TDOA) and/or frequency difference of arrival (FDOA). In this paper, the cluster flight orbit control law for SAMSON is discussed. The control law is aimed at regulating the mean semi-major axis, eccentricity and inclination so as to provide long-term bounded relative motion while utilizing small amount of fuel. The considered actuators are constant-thrust-magnitude thrusters. Simulations for 1 year are shown, validating the potential implementability of the proposed algorithm on-board the SAMSON satellites.

I. Introduction

Disaggregated satellites constitute an emerging concept in the realm of distributed space systems. The main idea is to replace a monolithic satellite by multiple free-flying, physically-separated modules interacting through wireless cross-links. The disaggregated satellites concept enables novel space architectures that can potentially outperform the conventional monolithic architectures.

Unlike traditional satellite formation flying missions, in disaggregated systems, the modules do not necessarily have to operate in a tightly-controlled formation; instead, they are required to maintain the inter-module distances bounded (typically between 100 m and 100 km) for the entire mission lifetime. This concept is termed *cluster flight* [1].

One of the first cluster flight demonstration missions is the Space Autonomous Mission for Swarming and Geolocation with Nanosatellites (SAMSON). The SAMSON project is led by the Distributed Space Systems Lab (DSSL) at the Technion[2]. It includes the first-ever nanosatellite trio, and has two main goals: (1) demonstrate long-term autonomous cluster flight and (2) geolocate a radiating electromagnetic terrestrial source based on time difference of arrival (TDOA) and/or frequency difference of arrival (FDOA). The 3 nanosatellites will be launched into a low Earth orbit

*Doctoral Student, Distributed Space Systems Lab, Faculty of Aerospace Engineering. email: leomazal@techunix.technion.ac.il

†Associate Professor, Distributed Space Systems Lab, Faculty of Aerospace Engineering. email: pgurfil@technion.ac.il

(LEO) together, to form an autonomous cluster, which is required to hold inter-satellite distances ranging from 100 m to 250 km. The nanosatellites will perform relative orbital element corrections to satisfy the relative distance constraints based on GPS measurements. The planned lifetime for the mission is 1 year. Each of the three nanosatellites will be equipped with a single cold-gas thruster, providing a bang-off-bang thrust on the order of tens of millinewtons.

Without control forces, initially-close satellites will drift apart due to differential accelerations. It is thus imperative to derive effective control strategies for keeping the cluster operational with limited fuel budgets. In the absence of perturbations, equal semimajor axes guarantee bounded motion[3]. But in more realistic scenarios, the problem is more complicated. The most significant perturbations affecting low Earth-orbit satellites are the Earth oblateness and drag. Many works presented strategies to mitigate or avoid relative drifts among satellites subject to the main perturbations – see e.g. [4, 5, 6, 7] and references therein. Mazal and Gurfil[8] recently derived constraints on the relative states, which ensure bounded motion under zonal harmonics and drag, in the context of long-term cluster flight. Ref. [8] also introduced an algorithm to steer a cluster to the desired relative states assuming impulsive cooperative maneuvers. Mazal, Mingotti and Gurfil introduced the first cooperative optimal low-thrust constant-magnitude guidance law for cluster-establishment, considering bang-off-bang thrust profiles[9].

Since the SAMSON satellites are equipped with constant-magnitude thrusters, the current work presents a cluster-keeping algorithm designed considering these harsh technological constraint. This closed-loop control algorithm is described and assessed. Although the actual on-board control algorithm for SAMSON has not been finalized yet, it will likely be based on the principles described throughout the paper.

II. Global Decentralized Cluster-Keeping Strategy and Algorithm

Consider a cluster composed of N satellites. It is required to hold the distances between any two satellites i and j within prescribed upper and lower thresholds, i.e $D_{\min} \leq d_{ij}(t) \leq D_{\max}$. $d_{ij}(t) \triangleq \|\mathbf{r}_j(t) - \mathbf{r}_i(t)\|$ denotes the distance between the satellites i and j at any time t, and $\mathbf{r}_i$ and $\mathbf{r}_j$ represent the position vectors of satellites i and j respectively. Hence, the control logic of the entire cluster should simultaneously monitor $N(N-1)/2$ inter-satellite distances. Most approaches on formation and cluster flight deal with only two satellites, and thus a single distance to be considered. However, if $N = 3$ as in SAMSON, the problem becomes more complex as the number of distances to simultaneously control is three, $d_{12}(t)$, $d_{23}(t)$, $d_{31}(t)$.

Consider two satellites, i and j, orbiting the Earth, under natural perturbations. If they are initially moving in proximity, the inter-satellite distance $d_{ij}(t)$ will exhibit a pattern similar to that illustrated in Fig. 1.

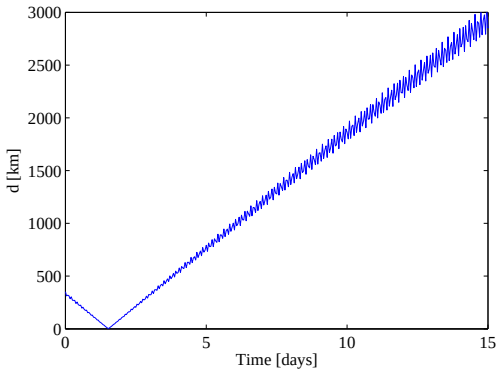

Figure 1: *Secular behavior of uncontrolled inter-satellite distance.*

In Fig. 1, one can distinguish a secular behavior superimposed with oscillations. The secular behavior reaches a minimum of ~ 0 km. The distance reaches a maximum at ~ 14000 km (in this example the semimajor axes of the satellites are ~ 7000 km). The maxima reached when when the angle between the position vectors of the satellites, denoted by η, satisfies $\eta \sim 180°$. Conversely, the minima are reached at times in which $\eta \sim 0°$.

The distance between the satellites can be written as

$$d_{ij}(t) = \sqrt{r_i^2(t) + r_j^2(t) - 2\, r_i(t)\, r_j(t)\, \cos\eta(t)} \tag{1}$$

where $r_i = \|\mathbf{r}_i\|$ and $r_j = \|\mathbf{r}_j\|$. For operational clusters in LEO, r_i and r_j are both bounded from above and below as $a_i(t)\,(1 - e_i(t)) \leq r_i(t) \leq a_i(t)\,(1 + e_i(t))$ and $a_j(t)\,(1 - e_j(t)) \leq r_j(t) \leq a_j(t)\,(1 + e_j(t))$. Yet, $d_{ij}(t)$ can attain very large or very small values if the angle $\eta(t)$ is not controlled. Furthermore, for practical scenarios of cluster flight, it holds that

$$\frac{\delta r(t)}{r_i(t)} = \frac{r_j(t) - r_i(t)}{r_i(t)} \ll 1 \tag{2}$$

Expanding Eq. (1) into a first-order Taylor series about $\frac{\delta r}{r_i} = 0$ yields

$$d(t) \simeq r_i(t)\sqrt{2}\sqrt{1 - \cos\left(\eta(t)\right)}\left(1 + \frac{1}{2}\frac{\delta r(t)}{r_i(t)}\right) \tag{3}$$

which shows the critical influence of η on the relative distance.

The main cause for the motion to seem locally-unbounded is a difference in the semimajor axes of the satellites, $\delta a_{ij} \triangleq a_i - a_j \neq 0$. Indeed, even in the unperturbed two-body problem, different semimajor axes lead to secular drifts of the distance between the satellites. For the perturbed two-body problem, the scenario is more complex, but still holding $\delta\overline{a}_{ij} \triangleq \overline{a}_i - \overline{a}_j > 0$ yields locally-unbounded secular behavior of $d_{ij}(t)$. In the presence of drag, different semimajor axes evolutions would affect the rate of the secular behavior. Generally speaking, for cluster flight purposes, these secular drifts must be avoided. However, they can also be exploited to hold the distances $d_{ij}(t)$ between the satellites of a cluster within given thresholds, as will be seen in the sequel.

To proceed, let $\overline{(\text{oe})}$ denote the mean value (secular component) of the orbital element (oe). It is well known that for mitigating the secular growth of the differential orbital elements $\delta\overline{\Omega}_{ij} \triangleq \overline{\Omega}_i - \overline{\Omega}_j$, $\delta\overline{\omega}_{ij} \triangleq \overline{\omega}_i - \overline{\omega}_j$, and $\delta\overline{M}_{ij} \triangleq \overline{M}_i - \overline{M}_j$ due to the J_2 effect, one could set $\delta\overline{a}_{ij} = \overline{a}_i - \overline{a}_j = 0$, $\delta\overline{e}_{ij} \triangleq \overline{e}_i - \overline{e}_j = 0$, and $\delta\overline{i}_{ij} \triangleq \overline{i}_i - \overline{i}_j = 0$[3]. However, in the presence of other effects such as differential drag, $\delta\overline{a}_{ij}$ is affected, leading to $\delta\overline{a}_{ij} \gtrless 0$ and thus a secular drift in the distance takes place. Assume that $\delta\overline{a}_{ij} > 0$, which implies the time that takes satellite i to complete one revolution is longer than that of satellite j. Thus, if satellite i is behind satellite j, they will get farther from each other, i.e. the angle η will grow. However, if due to a maneuver, $\text{sgn}(\delta\overline{a}_{ij})$ is inverted, satellite i will complete one revolution faster than satellite j. Consequently, they will start getting closer.

2.1 Global Strategy

The main strategy of the cluster control logic consists of performing corrective maneuvers, when at any time $t = t_i$ the inter-satellite distance between any two satellites of the cluster, $d_{ij}(t_i)$, reaches the upper or lower threshold. Recalling the secular behavior seen in Fig. 1, unless $\text{sgn}(\delta\overline{a}_{ij})$ is switched, it is expected that $d_{ij}(t) \quad \forall t > t_i$ will continue increasing. Thus, a control action aimed at switching $\text{sgn}(\delta a_{ij})$ must be performed. In case that $\overline{a}_i(t_i) > \overline{a}_j(t_i)$, the control logic performs a maneuver so that $\overline{a}_i^+ < \overline{a}_j^+$, where the superscript $(\text{oe})^+$ denotes the value of the orbital element (oe) immediately after the maneuver. Fig. 2 illustrates the idea, for an upper bound of 70 km.

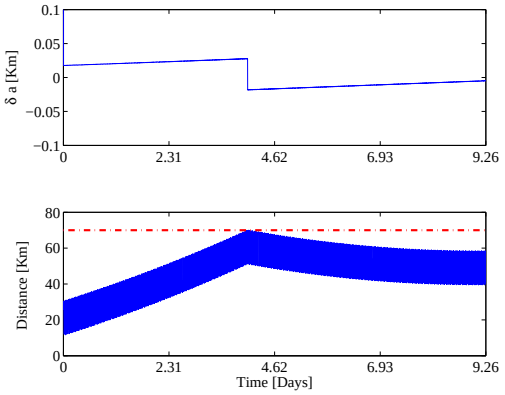

Figure 2: *Maneuvering switching the secular behavior of $d_{ij}(t)$.*

The differences in the semimajor axes after the maneuver, $\delta\overline{a}_{ij}^+ = \overline{a}_i^+ - \overline{a}_j^+$, are intended to be slightly different from zero, to properly affect the secular behavior of d_{ij}. However, they should not be too large, because the larger $|\delta\overline{a}_{ij}^+|$, the steeper the rate of the secular-like behavior. The goal of each collective maneuver will be to generate proper differences between the semimajor axes of the three satellites, such that the distances between any pair of satellites

are held within the given range.

When the cluster is composed of more than two satellites, the issue is more involved, because changes in one of the semimajor axes, say $\overline{a}_i$, affects the behavior of the distances between every pair of satellites involving satellite i, $d_{ij}(t) \quad \forall\ j \neq i$. For SAMSON, before performing a maneuver, a control logic properly sets $\overline{a}_i^+ \quad \forall i = 1 \ldots 3$, to obtain the desired behavior of $d_{ij}(t) \quad \forall\ i,\ j$ after the maneuver.

2.2 Defining Terminal States

This section shows how the terminal states of the satellites are determined, according to the states of the three satellites at $t = t_i$. The terminal states are the orbital elements that the satellites are steered to during the maneuver. Each time a maneuver is required this procedure takes place, setting the terminal states $\overline{e}^+$, $\overline{i}^+$, and $\overline{a}_k^+$ $k = 1, 2, 3$.

Assume that at t_i one of the three distances reached either the upper or the lower bound, and that $\overline{a}_k(t_i)$ are known. Without loss of generality, assume that $|d_{ij}(t_i) - D_M| > |d_{jk}(t_i) - D_M| > |d_{ki}(t_i) - D_M|$, where $D_M \triangleq (D_{\max} + D_{\min})/2$. Hence, it must hold that $d_{ij}(t_i)$ reached either the upper or the lower bound. Therefore, the first priority is to correct the secular behavior of d_{ij}, for which a constraint is imposed to switch the semimajor axes $\overline{a}_i$ and $\overline{a}_j$ as follows.

$$\begin{cases} \text{if } \overline{a}_i(t_i) > \overline{a}_j(t_i) & \Longrightarrow \quad \overline{a}_i^+ < \overline{a}_j^+ \\ \text{if } \overline{a}_i(t_i) < \overline{a}_j(t_i) & \Longrightarrow \quad \overline{a}_i^+ > \overline{a}_j^+ \end{cases} \tag{4}$$

Modifying $\overline{a}_i$ and $\overline{a}_j$ will also affect the behavior of d_{ik} and d_{jk}. Since $|d_{jk}(t_i) - D_M| > |d_{ki}(t_i) - D_M|$, $d_{jk}(t_i)$ is closer to one of the thresholds than $d_{ki}(t_i)$. Therefore, the second priority is to generate the proper secular behavior of $d_{jk}(t)$. To that end, the logic given in (6) yields a constraint between $\overline{a}_j^+$ and $\overline{a}_k^+$, where $\dot{\overline{d}}_{jk}$ denotes the secular rate of change of the distance d_{jk}.

With the constraints imposed to the pairs $(\overline{a}_i^+, \overline{a}_j^+)$ and $(\overline{a}_j^+, \overline{a}_k^+)$, it might suffice or not to completely sort the three terminal semimajor axes. For instance, if it was obtained that $\overline{a}_i^+ > \overline{a}_j^+$ and $\overline{a}_j^+ > \overline{a}_k^+$, then one concludes that $\overline{a}_i^+ > \overline{a}_j^+ > \overline{a}_k^+$. However, if $\overline{a}_i^+ > \overline{a}_j^+$ and $\overline{a}_j^+ < \overline{a}_k^+$ is obtained, either $\overline{a}_i^+ > \overline{a}_k^+ > \overline{a}_j^+$ or $\overline{a}_k^+ > \overline{a}_i^+ > \overline{a}_j^+$ are admissible. Thus, only in case that with the two constraints, (4) and (6), the terminal semimajor axes cannot be completely sorted because there are still two options, the logic (7) establishes a constraint between $\overline{a}_k^+$ and $\overline{a}_i^+$.

Applying the logic described in (4), (6), and (7), the terminal semimajor axes are properly sorted, such that it prevents the most critical distance d_{ij} from exceeding the allowed lower and upper bounds, as well as moving d_{jk} and d_{ki} away from the bounds.

To obtain slight differences in the semimajor axes, $\delta\overline{a}_{ij}^+ \quad \forall\ i, j$, the control logic proceeds in the following manner. First $(\text{oe})_p$ is defined and computed as

$$(\text{oe})_p \triangleq \frac{\max\left(\overline{(\text{oe})}_1(t_i), \overline{(\text{oe})}_2(t_i), \overline{(\text{oe})}_3(t_i)\right)}{2} + \frac{\min\left(\overline{(\text{oe})}_1(t_i), \overline{(\text{oe})}_2(t_i), \overline{(\text{oe})}_3(t_i)\right)}{2} \tag{5}$$

where (oe) stands for a, e, and i. Then, according to how the terminal semimajor axes were sorted, the satellite required to have the highest semimajor axis is steered to $\overline{a}^+ = a_p + \Delta a$; the satellite required to have the lowest semimajor axis is steered to $\overline{a}^+ = a_p - \Delta a$; and the satellite required to have a semimajor axis in between the former is steered to $\overline{a}^+ = a_p$. Δa is a positive user-defined parameter that affects the long-term performance of the algorithm. The larger Δa, the steeper are the secular drifts. However, if Δa is small, due to the tolerances of implementation, it might occur that in the end of the maneuver the constraints (4), (6), and (7) are not satisfied.

On the other hand, the eccentricities $\overline{e}_k$ are steered to $\overline{e}^+ = e_p$ and the inclinations $\overline{i}_k$ are steered to $\overline{i}^+ = i_p$, $k = 1, 2, 3$.The mean inclinations of the satellites are steered to an equal terminal state to avoid large out-of-plane separations.

$$\begin{cases} \text{if } d_{jk}(t_i) - D_M > (<)0 \text{ and } \dot{\overline{d}}_{jk} > (<)0 \text{ and } \overline{a}_j(t_i) > \overline{a}_k(t_i) & \Longrightarrow \quad \overline{a}_j^+ < \overline{a}_k^+ \\ \text{if } d_{jk}(t_i) - D_M > (<)0 \text{ and } \dot{\overline{d}}_{jk} < (>)0 \text{ and } \overline{a}_j(t_i) > \overline{a}_k(t_i) & \Longrightarrow \quad \overline{a}_j^+ > \overline{a}_k^+ \\ \text{if } d_{jk}(t_i) - D_M > (<)0 \text{ and } \dot{\overline{d}}_{jk} > (<)0 \text{ and } \overline{a}_j(t_i) < \overline{a}_k(t_i) & \Longrightarrow \quad \overline{a}_j^+ > \overline{a}_k^+ \\ \text{if } d_{jk}(t_i) - D_M > (<)0 \text{ and } \dot{\overline{d}}_{jk} < (>)0 \text{ and } \overline{a}_j(t_i) < \overline{a}_k(t_i) & \Longrightarrow \quad \overline{a}_j^+ < \overline{a}_k^+ \end{cases} \tag{6}$$

$$\begin{cases} \text{if } d_{ki}(t_i) - D_M > (<)0 \text{ and } \dot{\overline{d}}_{ki} > (<)0 \text{ and } \overline{a}_k(t_i) > \overline{a}_i(t_i) & \Longrightarrow \quad \overline{a}_k^+ < \overline{a}_i^+ \\ \text{if } d_{ki}(t_i) - D_M > (<)0 \text{ and } \dot{\overline{d}}_{ki} < (>)0 \text{ and } \overline{a}_k(t_i) > \overline{a}_i(t_i) & \Longrightarrow \quad \overline{a}_k^+ > \overline{a}_i^+ \\ \text{if } d_{ki}(t_i) - D_M > (<)0 \text{ and } \dot{\overline{d}}_{ki} > (<)0 \text{ and } \overline{a}_k(t_i) < \overline{a}_i(t_i) & \Longrightarrow \quad \overline{a}_k^+ > \overline{a}_i^+ \\ \text{if } d_{ki}(t_i) - D_M > (<)0 \text{ and } \dot{\overline{d}}_{ki} < (>)0 \text{ and } \overline{a}_k(t_i) < \overline{a}_i(t_i) & \Longrightarrow \quad \overline{a}_k^+ < \overline{a}_i^+ \end{cases} \tag{7}$$

The rationale behind the computation of $(\text{oe})_p$ is to minimize the largest required element variation, i.e.

$$(\text{oe})_p = \min_{(\text{oe})} \max \begin{bmatrix} |\overline{(\text{oe})}_1(t_i) - (\text{oe})| \\ |\overline{(\text{oe})}_2(t_i) - (\text{oe})| \\ |\overline{(\text{oe})}_3(t_i) - (\text{oe})| \end{bmatrix}^{\text{T}} \tag{8}$$

2.3 Control Law for Reaching the Terminal States

Assume that at time $t = t_i$ the satellite k have mean elements $\overline{a}_k(t_i)$, $\overline{e}_k(t_i)$ and $\overline{i}_k(t_i)$, $k = 1, 2, 3$. It is desired to steer the satellite such that at the end of maneuver it reaches $\overline{a}_k^+$, $\overline{e}^+$ and $\overline{i}^+$.

Define the satellite-fixed frame $\mathcal{V}_k$ as follows: The $\hat{X}_k$ direction lies along the instantaneous velocity vector $\mathbf{v}_k$, the $\hat{Z}_k$ direction lies along the instantaneous angular momentum vector $\mathbf{h}_k = \mathbf{r}_k \times \mathbf{v}_k$, and $\hat{Y}_k$ completes the right-handed triad.

Assume that each satellite is equipped with a single engine that exerts constant-magnitude thrust T_k. Defining α_k and δ_k as the respective right ascension and declination angles, with respect to the frame $\mathcal{V}_k$, the thrust vector is resolved in $\mathcal{V}_k$ as

$$\mathbf{T}_k = T_k \begin{bmatrix} \cos(\alpha_k)\cos(\delta_k) \\ \sin(\alpha_k)\cos(\delta_k) \\ \sin(\delta_k) \end{bmatrix} \tag{9}$$

To design a control law for α_k and δ_k that steers the system to the desired state, the following Lyapunov function is defined:

$$V_k = \frac{1}{2} \begin{bmatrix} \overline{a}_k - \overline{a}_k^+ \\ \overline{e}_k - \overline{e}^+ \\ \overline{i}_k - \overline{i}^+ \end{bmatrix}^{\text{T}} \begin{bmatrix} k_a & 0 & 0 \\ 0 & k_e & 0 \\ 0 & 0 & k_i \end{bmatrix} \begin{bmatrix} \overline{a}_k - \overline{a}_k^+ \\ \overline{e}_k - \overline{e}^+ \\ \overline{i}_k - \overline{i}^+ \end{bmatrix} \tag{10}$$

Differentiating V_k yields

$$\dot{V}_k = k_a(\overline{a}_k - \overline{a}_k^+)\dot{\overline{a}}_k + k_e(\overline{e}_k - \overline{e}^+)\dot{\overline{e}}_k + k_i(\overline{i}_k - \overline{i}^+)\dot{\overline{i}}_k \tag{11}$$

For any orbital element (oe), the time derivative of its secular behavior $\dot{\overline{(\text{oe})}}$ can be written as

$$\dot{\overline{(\text{oe})}} = \dot{\overline{(\text{oe})}}_p + \dot{\overline{(\text{oe})}}_c \tag{12}$$

where the sub-index $(\cdot)_p$ denotes variations due to natural perturbations and $(\cdot)_c$ denotes variations due to control actions.

It is important to stress that the maneuvers usually last for short time intervals, shorter than an orbital period, and thus the effect of perturbations during the maneuver is small. Yet, the effects due to Earth oblateness (mainly the J_2 term) are taken into account during the maneuvers. Under J_2 perturbations, $\dot{\overline{a}}_{k_p} = \dot{\overline{e}}_{k_p} = \dot{\overline{i}}_{k_p} = 0$. Thus, the terms remaining to be computed are $\dot{\overline{(\text{oe})}}_c$. According to Ref. [10] the effect of the control thrust on the mean elements can be approximated by the effect of the same thrust on the corresponding osculating elements. The Gauss Variational Equations

(GVE) resolved in the frame $\mathcal{V}$ are given by[11]

$$\dot{\bar{a}}_k = \frac{2\,a_k^2\,v_k}{m_k\,\mu} T_k \cos(\alpha_k)\cos(\delta_k) \tag{13}$$

$$\begin{aligned}\dot{\bar{e}}_k = &\frac{T_k\cos(\delta_k)}{v_k\,m_k} 2\,(e_k+\cos f_k)\cos(\alpha_k)\\ &-\frac{T_k\cos(\delta_k)}{v_k\,m_k}\frac{r_k}{a_k}\sin f_k\,\sin(\alpha_k)\end{aligned} \tag{14}$$

$$\dot{\bar{i}}_k = \frac{r_k}{h_k\,m_k}\cos\left(f_k+\omega_k\right) T_k \sin(\delta_k) \tag{15}$$

where v_k is the norm of the inertial velocity vector, m_k is the mass, f_k is the true anomaly, ω_k is the argument of perigee, and h_k is the norm of the angular momentum vector, all corresponding to satellite k.

Introducing Eqs. (13)-(15) into Eq. (11) yields

$$\dot{V}_k = \frac{T_k}{m}\left[\begin{array}{l}\beta_{1k}\,\cos\alpha_k\,\cos\delta_k + \beta_{2k}\,\sin\alpha_k\,\cos\delta_k\\ +\,\beta_{3k}\,\sin\delta_k\end{array}\right] \tag{16}$$

where

$$\begin{aligned}\beta_{1k} = &\,k_a(\bar{a}_k-\bar{a}_k^+)\frac{2\,a_k^2\,v_k}{\mu}\\ &+k_e(\bar{e}_k-\bar{e}^+)\frac{2\,(e_k+\cos f_k)}{v_k}\end{aligned} \tag{17}$$

$$\beta_{2k} = k_e(\bar{e}_k-\bar{e}^+)\frac{r_k\,\sin f_k}{a_k\,v_k} \tag{18}$$

$$\beta_{3k} = k_i(\bar{i}_k-\bar{i}^+)\frac{r_k\,\cos\left(f_k+\omega_k\right)}{h_k} \tag{19}$$

In order to guarantee that $\dot{V}$ will be always negative at any point different from the desired one, α and δ are selected as

$$(\alpha_k^*,\,\delta_k^*) = \arg\min_{(\alpha_k,\,\delta_k)}\begin{bmatrix}\beta_{1k}\\ \beta_{2k}\\ \beta_{3k}\end{bmatrix}^{\mathrm{T}}\begin{bmatrix}\cos\alpha_k\,\cos\delta_k\\ \sin\alpha_k\,\cos\delta_k\\ \sin\delta_k\end{bmatrix} \tag{20}$$

It can be proved that for any value of β_{1k}, β_{2k}, and β_{3k}, the minimum of $\dot{V}$ will be negative, unless $\beta_{1k}=\beta_{2k}=\beta_{3k}=0$ in which case $\dot{V}_k=0$. However, β_{1k}, β_{2k}, and β_{3k} will simultaneously vanish *and remain* zero only for $(\bar{a}_k-\bar{a}_k^+)=(\bar{e}_k-\bar{e}^+)=(\bar{i}_k-\bar{i}^+)=0$, which is the desired terminal condition.

The global minimum of $\dot{V}_k$ is found either at

$$\begin{cases}\alpha_k^{1*} = \arctan\left(\dfrac{\beta_{2k}}{\beta_{1k}}\right)\\ \delta_k^{1*} = \arctan\left(\dfrac{\beta_{3k}}{\beta_{1k}\cos\alpha_k^{1*}+\beta_{2k}\sin\alpha_k^{1*}}\right)\end{cases} \tag{21}$$

or at

$$\begin{cases}\alpha_k^{2*} = \alpha_k^{1*}+\pi\\ \delta_k^{2*} = -\delta_k^{1*}\end{cases} \tag{22}$$

For given β_{1k}, β_{2k}, β_{3k}, if the minimum is found at $\left(\alpha_k^{1*},\,\delta_k^{1*}\right)$ and it attains a value $\dot{V}_k(\alpha_k^{1*},\,\delta_k^{1*})<0$, then the maximum is found at $\left(\alpha_k^{2*},\,\delta_k^{2*}\right)$ attaining $\dot{V}_k(\alpha_k^{2*},\,\delta_k^{2*}) = -\dot{V}_k(\alpha_k^{1*},\,\delta_k^{1*})>0$.

2.3.1 Implementation Issues

Actual implementation of this control law requires to define tolerances to terminate the maneuver. Generally speaking, these tolerances generate a trade-off between the accuracy in the results of the maneuver and required fuel. The user should select them in such a way that they generate good performances without demanding too large fuel amounts for each maneuver.

In the control strategy of the whole cluster, the terminal desired elements $\bar{a}_k^+$, $\bar{e}^+$, $\bar{i}^+$ are computed at time $t=t_i$, once the necessity of the maneuver was detected. Since then, each satellite is required to maneuver until certain terminal conditions are achieved. Two different approaches can be considered to define the termination of the maneuver of each satellite.

The *first approach* is that each satellite k executes its maneuver until it achieves $|\bar{a}_k-\bar{a}_k^+|<\varepsilon_a$, $|\bar{e}_k-\bar{e}^+|<\varepsilon_e$, and $|\bar{i}_k-\bar{i}^+|<\varepsilon_i$, for some positive constants ε_a, ε_e, ε_i. Once these conditions are achieved, the satellite switches off its thruster and continues coasting. This approach presents two main drawbacks. The first is that it might lead to unbalanced fuel consumption. If the maneuvering times required for the three satellites are different, it might generate mass differences, and consequently differences in the ballistic coefficient, which is undesirable due to differential drag effects. Another disadvantage is that if the maneuver time is different, by the time that the last satellite completes its maneuver, the orbital elements of the other satellites

might undergo variations with respect to the desired terminal elements, thus preventing the system from achieving the desired terminal conditions simultaneously.

The *second approach* imposes the same maneuver time for all the satellites of the cluster. Thus, instead of terminal conditions for each satellite, there is a single collective terminal condition requiring that the collective maneuver is terminated once

$$\begin{aligned} &|\overline{a}_k - \overline{a}_k^+| < \varepsilon_a \text{ and } |\overline{e}_k - \overline{e}^+| < \varepsilon_e \\ &\text{and } |\overline{i}_k - \overline{i}^+| < \varepsilon_i \quad \forall k \end{aligned} \tag{23}$$

The advantages of this approach is that the mass consumption of the three satellites is the same, provided that the thrust-level exerted by each engine is the same - which is the design assumption. Moreover, once the maneuver is terminated, all the satellites have the required terminal orbital elements up to the allowed tolerances. However, there is an important drawback to be considered. Assume that satellite 1 already reached its desired orbital elements, i.e. it is within the required tolerances while satellite 2 has not yet achieved the terminal state. Satellite 1 will undergo a chattering process in α_1 and δ_1 while attempting to track the desired terminal orbital elements. This chattering process might constitute an involved issue that the attitude control system should cope with.

Another difficulty inherent to any of these approaches is the selection of the gains k_a, k_e, and k_i. While some k_a, k_e, and k_i work efficiently for some set of initial conditions, it might happen that there are not proper for another set of initial conditions. Although for any set of positive k_a, k_e, and k_i the control law will ensure convergence to the desired terminal values, the time of convergence and the mass consumption will vary for different selections of gains. Therefore, exhaustive tests should be performed to find gains that work efficiently for the most likely initial conditions.

Next, an example of a single maneuver is illustrated to stress the behavior of the designed control law. Figs. 3 and 4 depict the evolution of the maneuver for three satellites, with initial conditions given in Table 1.

In Fig. 3, the evolution of the orbital elements $\overline{a}_k(t)$, $\overline{e}_k(t)$, $\overline{i}_k(t)$, and the masses $m_k(t)$, $k = 1, 2, 3$ are shown. The terminal condition was achieved after 2 minutes, and the maneuver was terminated. Considering a thrust $T_k = 80$ mN. and Isp $= 60$ sec., the mass consumption was about 17 grams. With respect to the semi-major axes, the maneuver was aimed at setting that $\overline{a}_3^+ > \overline{a}_2^+ > \overline{a}_1^+$. Moreover, $\Delta a = 0.005$ km., and $\varepsilon_a = 0.002$ km., $\varepsilon_e = 0.0001$ km., and $\varepsilon_i = 0.025$ deg. The various curves in each plot are referred to each satellite, 1, 2, 3, and the dash-dot lines denoted by p refer to a_p, e_p, and i_p respectively. In Fig. 4, the Lyapunov function $V(t) = V_1(t) + V_2(t) + V_3(t)$, and the angles $\alpha_k(t)$ and $\delta_k(t)$ are plotted.

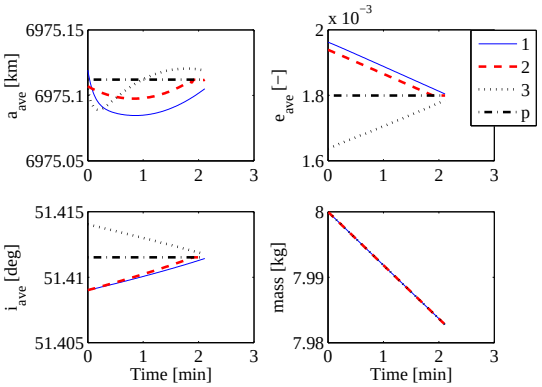

Figure 3: *Evolution of the orbital elements and mass during a maneuver.*

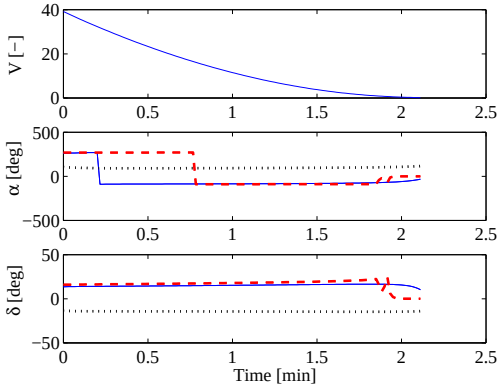

Figure 4: *Control angles and Lyapunov function during a maneuver.*

During the former simulation, the equations of motion were written as

$$
\begin{aligned}
\dot{\mathbf{r}}_k &= \mathbf{v}_k \\
\dot{\mathbf{v}}_k &= -\mu \frac{\mathbf{r}_k}{\|\mathbf{r}_k\|^3} \\
&\quad - \frac{\mu\, J_2\, R_q^2}{2\,\|\mathbf{r}_k\|^5} \left(6 \begin{bmatrix} 0 \\ 0 \\ z_k \end{bmatrix} + \left[3 - 15 \left(\frac{z_k}{\|\mathbf{r}_k\|} \right)^2 \right] \mathbf{r}_k \right) \\
&\quad + \mathcal{D}_{\mathcal{E}}^{\mathcal{V}_k} \frac{\mathbf{T}_k}{m_k} \\
\dot{m}_k &= -\frac{T_k}{I_{sp}\, g_0}
\end{aligned}
\tag{24}
$$

where $\mathbf{T}_k$ was given according to (9), and $\mathcal{D}_{\mathcal{E}}^{\mathcal{V}_k}$ is the direction cosine matrix transforming any vector in $\mathcal{V}_k$ into the same vector resolved in the Earth-centered inertial frame, $\mathcal{E}$. Moreover, $\mathbf{v}_k$ is the velocity vector in the $\mathcal{E}$ frame, R_q is the Equatorial radius of the Earth, J_2 is the coefficient of the first term in the zonal harmonics geopotential, μ is the gravitational parameter, and g_0 is the gravitational acceleration at sea-level. To implement the mean orbital elements feedback, the inertial position $\mathbf{r}_k$ and the inertial velocity $\mathbf{v}_k$ were first transformed into the osculating orbital elements; to obtain the required mean elements, the first-order mapping between mean and osculating elements presented in Ref. [10] was utilized.

2.4 Long-Term Simulation

This section shows an example of the global cluster-keeping algorithm explained above. In this example, the cluster consists of 3 satellites, each of which is equipped with a $T_k = 80$ mN thruster, and Isp = 60 sec. The initial mass is $m_k(t_0) = 7.98$ kg. The required parameters were set as $\Delta a = 0.005$ km., $\varepsilon_a = 0.002$ km., $\varepsilon_e = 0.0002$, and $\varepsilon_i = 0.025$ deg. The simulation was initialized with the initial conditions detailed in Table 2, and was performed for an interval of 1 year, which is the planned lifetime for the SAMSON project.

The overall behavior of the cluster is shown in Fig. 5.

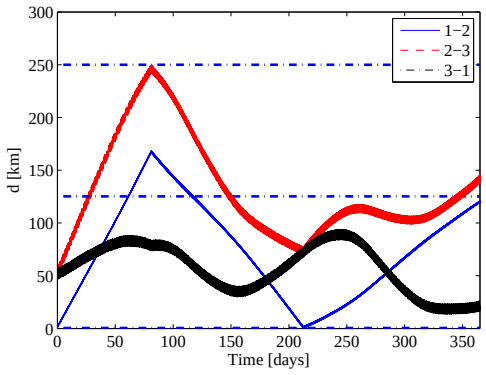

Figure 5: *Characteristic behavior of uncontrolled inter-satellite distance.*

Figure 5 shows the three inter-satellite distances $d_{12}(t)$, $d_{23}(t)$, and $d_{31}(t)$. They are held within the bounds because the maneuvers are performed properly. At $t_i = 80.96$ days, $d_{23}(t_i)$ reaches the upper bound, and thus a maneuver is executed. Before the maneuver, the semimajor axes were $\overline{a}_1(t_i) = 6973.512$ km, $\overline{a}_2(t_i) = 6973.528$ km, and $\overline{a}_3(t_i) = 6973.515$ km. According to Eqs. (4), (6) and (7), the terminal semimajor axes after the maneuver should satisfy $\overline{a}_1^+ > \overline{a}_3^+ > \overline{a}_2^+$. The maneuver achieves this requirement and the cluster is held within the bounds. At $t_i = 212.4$ days a new maneuver is required as $d_{12}(t_i)$ reaches the lower threshold. Before the maneuver, the semimajor axes were $\overline{a}_1(t_i) = 6969.454$ km, $\overline{a}_2(t_i) = 6969.443$ km, and $\overline{a}_3(t_i) = 6969.447$ km. According to (4)-(7), the terminal semimajor axes after the maneuver should satisfy $\overline{a}_2^+ > \overline{a}_1^+ > \overline{a}_3^+$. The new maneuver achieves this requirement and the cluster is held within the bounds. After the two corrective maneuvers, the total mass consumption was 10.5 grams. For this example the propagation of the satellite orbits between maneuvers was performed by using an astrodynamical model including gravitational geopotential up to degree and order 21, drag according to the Jacchia-Roberts model, solar radiation pressure, and lunisolar attraction. The cross-sectional area of the satellites was assumed to be 0.1 m^2.

III. Conclusions

The cluster flight control method presented herein is simple, which makes it feasible for onboard autonomous implementation. The orbit control law for each satellite is robust in the sense that even if the thrust level were lower than the nominal value, it would take longer to reach the required terminal conditions, but eventually they would be attained. Even different ballistic coefficients would not represent a hard obstacle for the algorithm, as these possible differences would simply increase the frequency of the corrective maneuvers. Since the control strategy does not rely on very accurate targeting of the terminal conditions, unmodeled perturbations can still be rejected. Finally, the proposed algorithm could be easily extended to a larger number of satellites.

IV. Acknowledgements

This work was supported by the European Research Council Starting Independent Researcher Grant - 278231: Flight Algorithms for Disaggregated Space Architectures (FADER), the Ministry of Science of the State of Israel, and the Technion Graduate Fellowship Program.

Table 1: *Initial orbital elements for satellite 1 (row 1), 2 (row 2), and 3 (row 3).*

Satellite	a [km]	e [-]	i [deg]	Ω [deg]	ω [deg]	f [deg]	m [kg]
#1 @ (t_0)	6978.966	0.001704	51.422	293.492	62.185	273.643	8
#2 @ (t_0)	6978.952	0.001665	51.422	293.489	63.813	272.008	8
#3 @ (t_0)	6979.016	0.001253	51.427	293.475	75.330	260.951	8

Table 2: *Initial orbital elements for satellite 1 (row 1), 2 (row 2), and 3 (row 3).*

Satellite	a [km]	e [-]	i [deg]	Ω [deg]	ω [deg]	f [deg]	m [kg]
#1 @ (t_0)	6979.984	0.001717	51.427	293.489	57.302	286.349	7.98
#2 @ (t_0)	6979.997	0.001688	51.427	293.486	58.785	284.857	7.98
#3 @ (t_0)	6980.023	0.001550	51.428	293.474	69.065	275.033	7.98

IV. References

[1] Brown, O. and Eremenko, P., "Fractionated Space Architectures: A Vision for Responsive Space," *4th Responsive Space Conference*, Los Angeles, CA, 2006.

[2] Gurfil, P., Herscovitz, J., and Pariente, M., "The SAMSON Project - Cluster Flight and Geolocation with Three Autonomous Nano-satellites," *26th AIAA/USU Conference on Small Satellites*, Salt Lake City, UT, 2012.

[3] Alfriend, K., Vadali, S., Gurfil, P., How, J., and Breger, L., *Spacecraft Formation Flying: Dynamics,Control and Navigation*, Elseiver, Oxford, UK, 2010, Chapter 2, pp. 24, 35-36.

[4] Vadali, S. R., Schaub, H., and Alfriend, K. T., "Initial Conditions and Fuel-Optimal Control for Formation Flying of Satellites," *AIAA Guidance, Navigation, and Control Conference and Exhibit*, Portland, OR, 1999.

[5] Schaub, H. and Alfriend, K., "J_2 Invariant Relative Orbits for Spacecraft Formations," *Celestial Mechanics and Dynamical Astronomy*, Vol. 79, No. 2, February 2001.

[6] Mishne, D., "Formation Control of Satellites Subject to Drag Variations and J_2 Perturbations," *Journal of Guidance, Control and Dynamics*, Vol. 27, No. 4, July-August 2004, pp. 685–692.

[7] Beigelman, I. and Gurfil, P., "Optimal Fuel-Balanced Impulsive Formationkeeping for Perturbed Spacecraft Orbits," *Journal of Guidance, Control and Dynamics*, Vol. 31, No. 5, September-October 2008, pp. 1266–1283.

[8] Mazal, L. and Gurfil, P., "Cluster Flight Algorithms for Disaggregated Satellites," *Journal of Guidance, Control and Dynamics*, Vol. to appear, 2012.

[9] Mazal, L., Mingotti, G., and Gurfil, P., "Continuous-Thrust Cooperative Guidance Law for Disaggregated Satellites," *AIAA/AAS Astrodynamics Specialist Conference*, Minneapolis, MN, 2012, paper AIAA-2012-4742.

[10] Schaub, H. and Junkins, J., *Analytical mechanics of space systems*, Vol. 1, Aiaa, 2003, Chapter 14, pp. 731.

[11] Battin, R., *An Introduction to the Mathematics and Methods of Astrodynamics, Revised Edition*, AIAA Education Series, 1999, Chapter 10, pp. 489.